Electronic Structure of Ruthenium Cumulene Complexes $[Cl(PH_3)_4RuC_nH_2]^+$ ($n = 1-8$) and of Their Reduced States. Bonding and Properties of the Cationic, Neutral, and Anionic Series with Respect to the Cumulenic Chain Length

Nathalie Auger,[†] Daniel Touchard,[‡] Stéphane Rigaut,[‡] Jean-François Halet,[†] and Jean-Yves Saillard*[,†]

Laboratoire de Chimie du Solide et Inorganique Moléculaire, UMR-6511, Institut de Chimie de Rennes, Université de Rennes 1, 35042 Rennes Cedex, France, and Laboratoire de Chimie de Coordination et de Catalyse, UMR-6509, Institut de Chimie de Rennes, Université de Rennes 1, 35042 Rennes Cedex, France

Received July 9, 2002

DFT calculations have been performed on the $[Cl(PH_3)_4RuC_nH_2]^+$, $Cl(PH_3)_4RuC_nH_2$, and $[Cl(PH_3)_4RuC_nH_2]^-$ ($n = 1-8$) series. Analysis of their optimized geometries and electronic structures allows complete rationalization of their bonding, thermodynamic stability, and reactivity. The theoretical results are in full agreement with the available experimental data on related ruthenium cumulene compounds.

Introduction

Conjugated hydrocarbon molecules and polymers have always attracted great interest from the whole community of chemists, due not only to their numerous potential physical and chemical properties but also to, on the more academic side, their peculiar electronic structures, especially with respect to the understanding of their stability and properties.[1] The modification of the properties and/or stability of a conjugated molecule can be done in many ways, a simple one being the incorporation of heteroatoms.[1b,e,2] From this point of view, it is noteworthy that several groups have recently developed a fast-growing chemistry of compounds made of unsaturated carbon wires of various sizes capped at one or two ends by organometallic ML_n units.[3−18] This class of compounds is currently attracting much attention, mainly in view of their potential use in catalysis[13,14]

* To whom correspondence should be addressed. E-mail: saillard@univ-rennes1.fr. Fax: (33) 2 99 38 34 87.

[†] Laboratoire de Chimie du Solide et Inorganique Moléculaire.

[‡] Laboratoire de Chimie de Coordination et de Catalyse.

(1) (a) Kraft, A.; Grimsdale, A. C.; Holmes, A. B. *Angew. Chem.* **1998**, *110*, 416; *Angew. Chem., Int. Ed.* **1998**, *37*, 403. (b) Müllen, K.; Wegner, G. *Electronic Materials: The Oligomer Approach*; Wiley-VCH: Weinheim, Germany, 1998. (c) Tour, J. M. *Acc. Chem. Res.* **2000**, *33*, 791. (d) Martin, R. E.; Diederich, F. *Angew. Chem.* **1999**, *11*, 1440; *Angew. Chem., Int. Ed.* **1999**, *38*, 1350. (e) *Handbook of Conducting Polymers*; Skotheim, T. A., Elsenbaumer, R. L., Reynolds, J. R., Eds.; Marcel Dekker: New York, 1998.

(2) (a) Roncali, J. *Chem. Rev.* **1997**, *97*, 173. (b) Hay, C.; Hissler, M.; Fischemaster, C.; Rault-Bertelot, J.; Toupet, L.; Nyulaszi, L.; Réau, R. *Chem. Eur. J.* **2001**, *7*, 4222.

(3) (a) Werner, H. *Chem. Commun.* **1997**, 903. (b) Bruce, M. I. *Chem. Rev.* **1998**, *98*, 2797. (c) Cardieno, V.; Gamasa, M. P.; Gimeno, J. *Eur. J. Inorg. Chem.* **2001**, 571. (d) Selegue, J. P. *Organometallics* **1982**, *1*, 217. (e) Bruce, M. I. *Chem. Rev.* **1991**, *91*, 197.

(4) Touchard, D.; Haquette, P.; Daridor, A.; Toupet, L.; Dixneuf, P. H. *J. Am. Chem. Soc.* **1994**, *116*, 11157.

(5) Touchard, D.; Haquette, P.; Romero, A.; Dixneuf, P. H. *Organometallics* **1998**, *17*, 3844.

(6) Rigaut, S.; Maury, O.; Touchard, D.; Dixneuf, P. H. *Chem. Commun.* **2001**, 373.

(7) (a) Rigaut, S.; Le Pichon, L.; Daran, J.-C.; Touchard, D.; Dixneuf, P. H. *Chem. Commun.* **2001**, 1206. (b) Guesmi, S.; Touchard, D.; Dixneuf, P. H. *Chem. Commun.* **1996**, 2773.

(8) Touchard, D.; Dixneuf, P. H. *Coord. Chem. Rev.* **1998**, *178−180*, 409.

(9) (a) Brady, M.; Weng, W.; Zhou, Y.; Seyler, J. W.; Amoroso, A. J.; Arif, A. M.; Böhme, M.; Frenking, G.; Gladysz, J. A. *J. Am. Chem. Soc.* **1997**, *119*, 775. (b) Paul, F.; Meyer, W.; Toupet, L.; Jiao, H.; Gladysz, J. A.; Lapinte, C. *J. Am. Chem. Soc.* **2000**, *122*, 9405. (c) Dembinski, R.; Bartik, T.; Bartik, B.; Jaeger, M.; Gladysz, J. A. *J. Am. Chem. Soc.* **2000**, 122, 810.

(10) (a) Gil-Rubio, J.; Laubender, M.; Werner, H. *Organometallics* **2000**, 19, 1365. (b) Hartbaum, C.; Mauz, Z.; Roth, G.; Weissenbach, K.; Fischer, H. *Organometallics* **1999**, *18*, 2619. (c) Wong, K. T.; Lehn, J.-M.; Peng, S. M.; Lee, G.-H. *Chem. Commun.* **2000**, 2259. (d) Hong, B.; Ortega, J. V. *Angew. Chem., Int. Ed.* **1998**, 37, 15. (e) McDonagh, A. M.; Humphrey, M. G.; Samoc, M.; Luther-Davies, B.; Houbrechts, S.; Wada, T.; Sasabe, H.; Persoons, A. *J. Am. Chem. Soc.* **1999**, *121*, 1405. (f) Esteruelas, M. A.; Gomez, A. V.; Lopez, A.; Modrego, J.; Oñate, E. *Organometallics* **1997**, *16*, 5826. (g) Cadierno, V.; Gamasa, M. P.; Gimeno, J.; González-Cueva, M.; Lastra, E.; Borge, J.; García-Granda, S.; Pérez-Carreño, E. *Organometallics* **1996**, *15*, 2137. (h) Kheradmandan, S.; Heinze, K.; Schmalle, H. W.; Berke, H. *Angew. Chem.* **1999**, *111*, 2412; *Angew. Chem., Int. Ed.* **1999**, *38*, 2270. (i) Fernandez, F. J.; Blacque, O.; Montserrat, A.; Berke, H. *Chem. Commun.* **2001**, 1266. (j) Ren, T.; Zou, G.; Alvarez, J. C. *Chem. Commun.* **2000**, 1197.

(11) Bruce, M. I.; Low, P. J.; Costuas, K.; Halet, J.-F.; Best, S. P.; Heath, G. A. *J. Am. Chem. Soc.* **2000**, *122*, 1949.

(12) Winter, R. F. *Eur. J. Inorg. Chem.* **1999**, 2121. Winter, R. F.; Hornung, F. M. *Organometallics* **1999**, *18*, 4005.

(13) (a) Grubbs, H.; Chang, S. *Tetrahedron* **1998**, *54*, 4413. (b) Bruneau, C.; Dixneuf, P. H. *Acc. Chem. Res.* **1999**, *32*, 311.

(14) (a) Furstner, A.; Picquet, M.; Bruneau, C.; Dixneuf, P. H. *Chem. Commun.* **1998**, 1315. (b) Picquet, M.; Bruneau, C.; Dixneuf, P. H. *Chem. Commun.* **1998**, 2249. (c) Fürstner, A.; Hill, A. F.; Liebl, M.; Wilton-Ely, J. D. E. T. *Chem. Commun.* **1999**, 615. (d) Picquet, M.; Touchard, D.; Bruneau, C.; Dixneuf, P. H. *New J. Chem.* **2000**, 141. (e) Osipov, S. N.; Artyushin, O. I.; Kolomiets, A. F.; Bruneau, C.; Picquet, M.; Dixneuf, P. H. *Eur. J. Org. Chem.* **2001**, 3891.

(15) (a) Paul, F.; Lapinte, C. *Coord. Chem. Rev.* **1998**, *178−180*, 431. (b) Martin, R. E.; Diederich, F. *Angew. Chem., Int. Ed. Engl.* **1999**, *38*, 1350. (c) Ward, M. D. *Chem. Ind.* **1996**, *15*, 568. (d) Ziessel, R.; Hissler, M.; El-Gayhouri, A.; Harriman, A. *Coord. Chem. Rev.* **1998**, *178−180*, 125. (e) Whittall, I. R.; McDonagh, A. M.; Humphrey, M. G. *Adv. Organomet. Chem.* **1999**, *43*, 349. (f) Stang, P. J.; Olenyuk, B. *Acc. Chem. Res.* **1997**, *30*, 502. (g) Kingsborough, R. P.; Swager, T. M. *Prog. Inorg. Chem.* **1999**, *48*, 123. (h) Nguyen, P.; Gómez-Elipe, P.; Manners, I. *Chem. Rev.* **1999**, *99*, 1515. (i) Wu, I. Y.; Lin, J. T.; Wen, Y. S. *Organometallics* **1999**, *18*, 320.

(16) Stang, P. J. *Chem. Eur. J.* **1998**, *4*, 19.

10.1021/om020543c CCC: $25.00
Publication on Web 03/13/2003

or as electronic devices in molecular engineering processes.[15−18] For these reasons, their electronic structures are also currently being investigated with the help of various quantum-chemical methods. [9a,11,19−23]

In this paper, we use density functional theory (DFT) to study the electronic structure of a series of ruthenium cumulene cations as well as their homologues reduced by one and two electrons. The simplified formulas $[Cl(PH_3)_4RuC_nH_2]^+$ ($n = 1-8$) have been chosen to model the $[X(dppe)_2RuC_nR_2]^+$ (X = Cl, PhCC; dppe = $P(Ph)_2(CH_2)_2P(Ph)_2$; R = Ph, CH_3) series, the chemistry of which has been developed by some of us.[4−8] So far, complexes up to $n = 5$ have been prepared.[4,5] Three of them have been characterized by X-ray diffraction, namely $[(PhCC)(dppe)_2RuC_3Ph_2]^+$, $[Cl(dppe)_2RuC_3(NEt_2)(CHCPh_2)]^+$, and $[Cl(dppe)_2RuC_5Ph_2]^+$.[4,5] It is noteworthy that all these complexes contain an odd number of carbon atoms in their cumulene chain, species bearing an even number of carbons appearing to be less stable. Cyclic voltammetry shows that the $[X(dppe)_2RuC_nR_2]^+$ 18-electron complexes can be reversibly reduced by one electron. Although no neutral species has been so far isolated, the $Cl(dppe)_2RuC_3R_2$ (R = Ph, CH_3) and $Cl(dppe)_2RuC_5Ph_2$ radicals centered on the carbon chain have been characterized by EPR spectroscopy and hydrogen capture reactions.[6]

We provide below a complete description of the bonding for this series of compounds as well as for their two reduced states. We analyze the variation of the electronic properties with respect to the cumulenic chain length, and we propose a rationalization of their electrochemical behavior and reactivity.

Computational Details

Density functional calculations were carried out using the Amsterdam density functional (ADF) program developed by Baerends and co-workers[24] using the local density approximation in the Vosko−Wilk−Nusair parametrization.[25] Nonlocal corrections for the exchange and for the electron correlation were performed using the Becke88 functional[26] for the exchange and the Perdew86 functional[27] for the correlation. The standard ADF STO basis set IV, of triple-ζ quality for the valence orbitals, was used for all the atoms. The frozen-core approximation was assumed.[28] The numerical integration procedure applied for the calculations was developed by te Velde et al.[29] The optimization procedures and calculations of the normal vibrational mode frequencies were carried out according to the method developed by Ziegler et al.[30] For all the open-shell systems, spin-polarized calculations were performed.

Results and Discussion

1. The 18-Electron $[Cl(PH_3)_4RuC_nH_2]^+$ Series. DFT calculations were carried out on the model series $[Cl(PH_3)_4RuC_nH_2]^+$ ($n = 1-8$; see Computational Details). Full geometry optimization without any symmetry constraint yielded geometries which can be described as slightly distorted ideal structures of C_{2v} symmetry, with the C_nH_2 plane lying in a staggered position with respect to the phosphine ligands. The origin of the slight distortion away from C_{2v} originates from steric repulsions between hydrogen atoms of the phosphine ligands. Thus, the RuC_n chains are almost perfectly linear, as exemplified by the optimized geometry of the $[Cl(PH_3)_4RuC_7H_2]^+$ model, which is shown in Figure 1.

The major computed bond distances of the $[Cl(PH_3)_4RuC_nH_2]^+$ cations are given in Figure 2. The optimized geometries exhibit structural trends similar to those previously computed on related isoelectronic complexes.[20,23] The Ru−C distances become longer when n increases, and they are longer for odd values of n than for even values of n. However, this difference between odd and even chains tends to vanish as n increases, with a common asymptotic Ru−C distance of ∼1.92 Å. This distance corresponds to a ruthenium−carbon double bond. The optimized geometries of $[Cl(PH_3)_4RuC_3H_2]^+$ and $[Cl(PH_3)_4RuC_5H_2]^+$ are in satisfying agreement with the X-ray molecular structures of $[Cl(dppe)_2RuC_3(NEt_2)(CHCPh_2)]^+$ and $[Cl(dppe)_2RuC_5Ph_2]^+$.[7,8] In these compounds, the sequence of the experimental bond distances (in Å) along the RuC_n chain (starting from Ru) are 1.962, 1.229, 1.409 and 1.900, 1.250, 1.300, 1.240, 1.360 for the former[7] and the latter,[8] respectively.

The MO diagrams of the $[Cl(PH_3)_4RuC_nH_2]^+$ series are shown in Figure 3, in which the HOMO and LUMO percentages of localization on the ruthenium atom and the C_n chain are also indicated. As expected, the HOMO/LUMO gap decreases as n increases. Some odd/even damped oscillation of this gap can also be noticed. The HOMO and LUMO localization of these MO's on the C_n chain increases with n.

The MO interactions between the $[Cl(PH_3)_4Ru]^+$ and the C_3H_2 and C_4H_2 fragments are schematically illustrated in parts a and b of Figure 4, for the $[Cl(PH_3)_4RuC_3H_2]^+$ and $[Cl(PH_3)_4RuC_4H_2]^+$ complexes, respectively. As a detailed bonding analysis within the related isoelectronic $(CO)_5CrC_nH_2$ series has been recently provided by Re et al.,[20a] we only briefly report here the main outlines. The π manifold of the planar C_nH_2 ligand can be divided into two categories: namely the MOs which are perpendicular to the C_nH_2 plane (labeled $\pi_\perp$) and those which lie in this plane ($\pi_\parallel$). There is no degeneracy between the $\pi_\perp$ and the $\pi_\parallel$ orbitals, since the

(17) (a) Fillaut, J.-L.; Price, M.; Johnson, A. L.; Perruchon, J. *Chem. Commun*. **2001**, 739. (b) Yam, V. W.-W., Tang, R. P.-L.; Wong, K. M.-C.; Cheung, K.-K. *Organometallics* **2001**, *20*, 4476.
(18) Hurst, S. K.; Cifuentes, M. P.; Morrall, J. P. L.; Lucas, N. T.; Whittall, I. R.; Humphrey, M. G.; Asselberghs, I.; Persoons, A.; Samoc, M.; Luther-Davies, B.; Willis, A. C. *Organometallics* **2001**, *20*, 4664.
(19) (a) Belanzoni, P.; Re, N.; Rosi, M.; Sgamellotti, A.; Floriani, C. *Organometallics* **1996**, *15*, 4264. (b) Belanzoni, P.; Re, N.; Sgamellotti, A.; Floriani, C. *J. Chem. Soc., Dalton Trans.* **1997**, 4773. (c) Belanzoni, P. B.; Re, N.; Sgamellotti, A.; Floriani, C. *J. Chem. Soc., Dalton Trans.* **1998**, 1825. (d) Belanzoni, P.; Sgamellotti, A.; Re, N.; Floriani, C. *Inorg. Chem*. **2000**, *39*, 1147.
(20) (a) Re, N.; Sgamellotti, A.; Floriani, C. *Organometallics* **2000**, *19*, 1115. (b) Marrone, A.; Re, N. *Organometallics* **2002**, *21*, 3562.
(21) Winter, R. F.; Klinkhammer; K. W.; Zalis, S. *Organometallics* **2001**, *20*, 1317.
(22) Koentjoro, O. F.; Rousseau, R.; Low, P. J. *Organometallics* **2001**, *20*, 4502.
(23) Jiao, H.; Gladysz, J. A. *New J. Chem*. **2001**, *25*, 551.
(24) Amsterdam Density Functional (ADF) Program, Release 2.0.1; Vrije Universiteit Amsterdam, Amsterdam, 1996.
(25) Vosko, S. D.; Wilk, L.; Nusair, M. *Can. J. Chem*. **1990**, 58, 1200.
(26) (a) Becke, A. D. *J. Chem. Phys*. **1986**, *84*, 4524. (b) Becke, A. D. *Phys. Rev. A* **1988**, *38*, 3098.
(27) Perdew, J. P. *Phys. Rev. B* **1986**, *33*, 8882. (b) Perdew, J. P. *Phys. Rev.* B **1986**, *34*, 7406.
(28) Baerends, E. J.; Ellis, D. E.; Ros, P. *Chem. Phys*. **1975**, *8*, 41.
(29) (a) Boerrigter, P. M.; te Velde, G.; Baerends, E. J. *Int. J. Quantum Chem*. **1988**, *33*, 87. (b) te Velde, G.; Baerends, E. *J. Comput. Phys*. **1992**, *99*, 84.
(30) Verluis, L.; Ziegler, T. *J. Chem. Phys*. **1988**, *88*, 322.

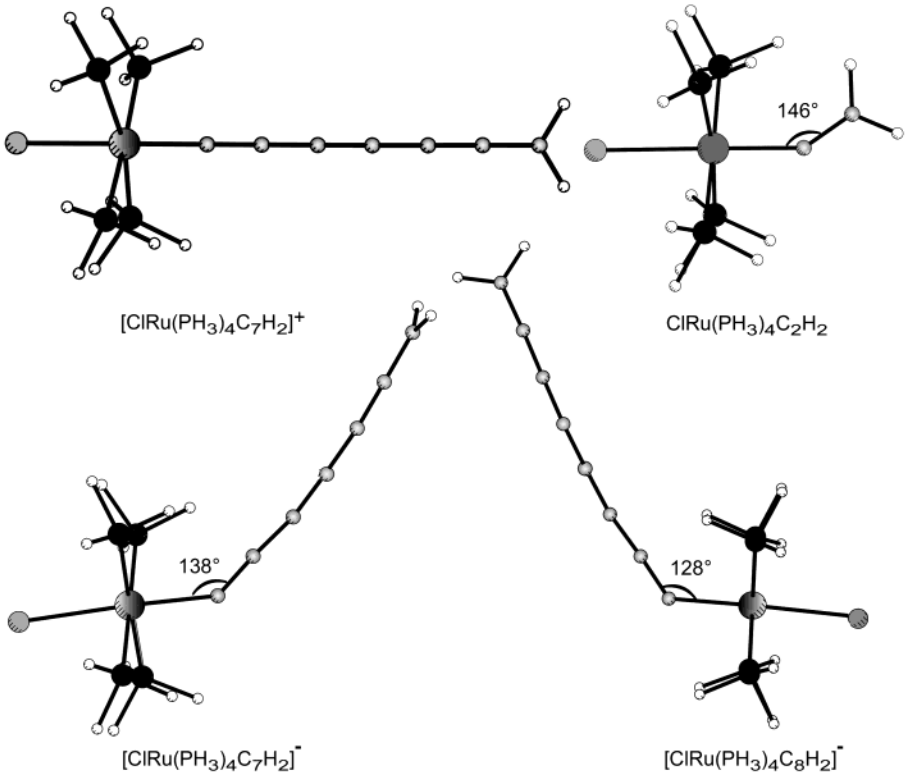

Figure 1. DFT-optimized geometry of $[Cl(PH_3)_4RuC_7H_2]^+$, $Cl(PH_3)_4RuC_2H_2$, $[Cl(PH_3)_4RuC_7H_2]^-$ ($S = 0$), and $[Cl(PH_3)_4RuC_8H_2]^-$ ($S = 0$).

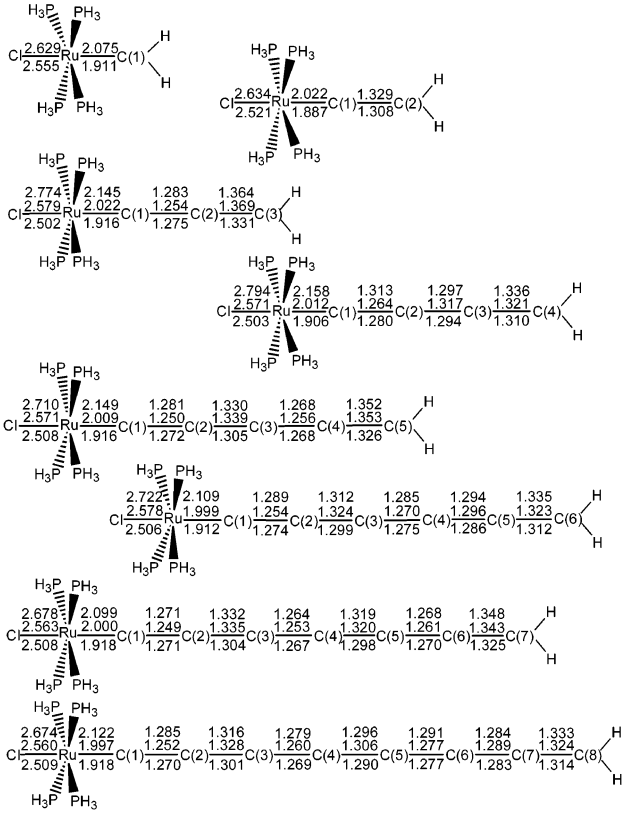

Figure 2. Major optimized bond lengths for the $[Cl(PH_3)_4RuC_nH_2]^{+/0/-}$ series: (bottom) cation; (middle) neutral species; (top) anion ($S = 0$). In the case of $n = 1, 2$, the anionic species were found to be unstable with respect to phosphine dissociation.

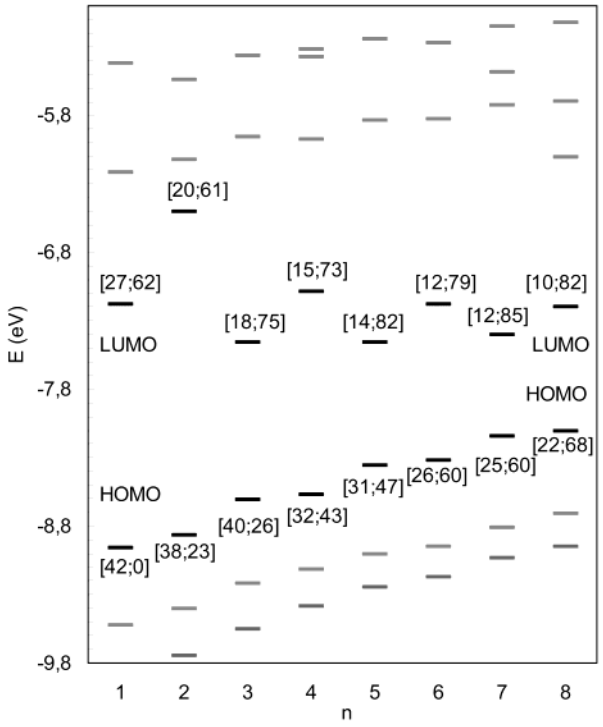

Figure 3. MO level ordering of the $[Cl(PH_3)_4RuC_nH_2]^+$ series. The percent contributions of the metal atom and the C_n chain to the HOMOs and LUMOs are given in brackets.

latter can mix with the hydrogen AOs while the former cannot. As a consequence of topology, when n is even, the HOMO and LUMO of C_nH_2 are $\pi_\perp$ and $\pi_{||}$, respectively. When n is odd, the opposite situation occurs. The ML_5-type $[Cl(PH_3)_4Ru]^+$ fragment has C_{4v} pseudosymmetry and therefore possesses two almost degenerate occupied π-type frontier molecular orbitals (FMO) of $\pi_\perp$

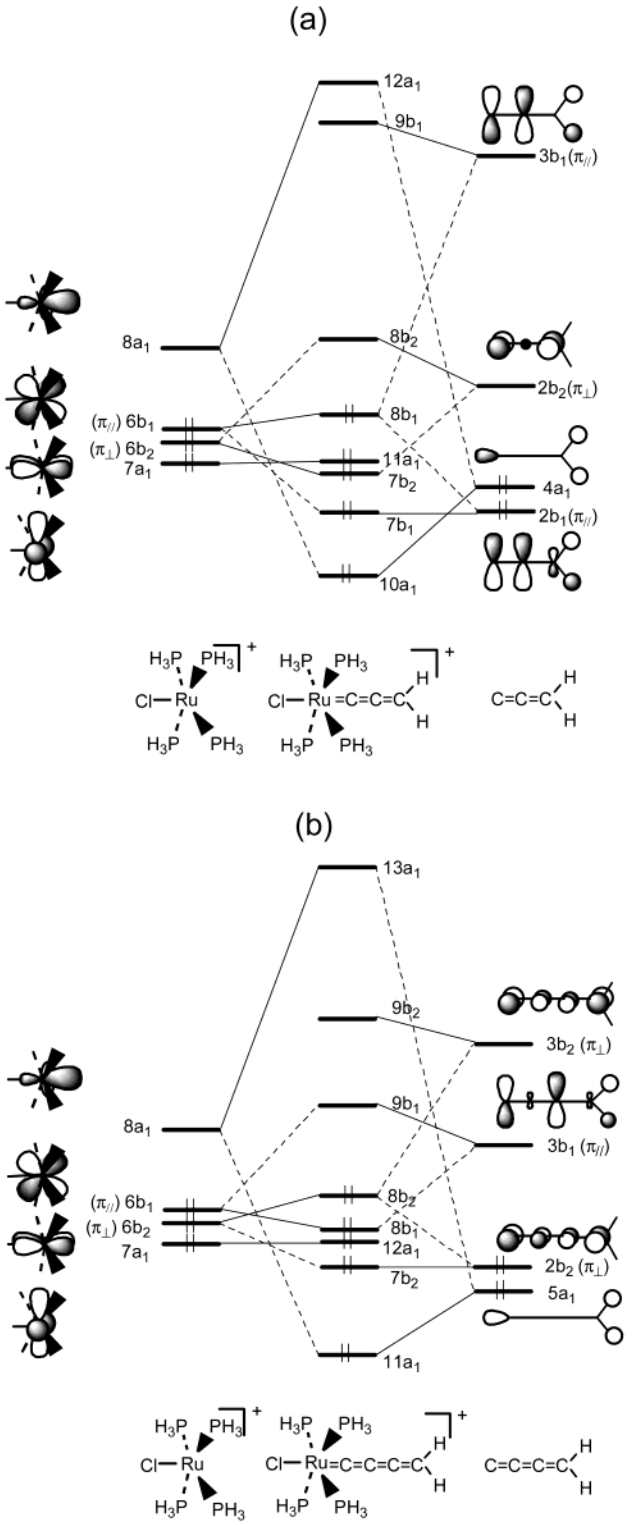

Figure 4. Qualitative orbital interaction diagrams for (a) $[Cl(PH_3)_4RuC_3H_2]^+$ and (b) $[Cl(PH_3)_4RuC_4H_2]^+$ complexes. Ideal C_{2v} symmetry is assumed.

and $\pi_{||}$ symmetries, which are the HOMOs of this fragment. One of them interacts in a destabilizing way (four-electron repulsion) with the C_nH_2 HOMO, and the other one interacts in a stabilizing way (two-electron attraction) with the LUMO of C_nH_2. To a first approximation the HOMO of a $[Cl(PH_3)_4RuC_nH_2]^+$ complex can be described as an antibonding combination of the HOMO of the C_nH_2 fragment and the same symmetry π-type HOMOs of the $[Cl(PH_3)_4Ru]^+$ fragment. Similarly, the LUMO of the $[Cl(PH_3)_4RuC_nH_2]^+$ complex can be roughly described as an antibonding combination of the LUMO of C_nH_2 with the other HOMO of the $Cl(PH_3)_4Ru^+$ fragment. Additional two-electron stabilization is provided by the interaction of the second LUMO of C_nH_2 with the metallic HOMO having the same symmetry. This MO analysis is exemplified for the $n = 3$, 4 cases by the diagrams of Figure 4.

Table 1. Decomposition of the Orbital Interaction Energy (E_{OI})[a] and Bond Dissociation Energy (BDE)[b] for the $[Cl(PH_3)_4RuC_nH_2]^+$ Series Corresponding to the Formation of the $[Cl(PH_3)_4Ru]^+$ and $[C_nH_2]$ Fragments (Values in kJ mol^{-1})

n	E_{Pauli}	$E_{electrostatic}$	E_{a1}	E_{a2}	E_{b1}	E_{b2}	E_{OI}	BDE
1	888	−840	−270	1	−28	−241	−538	−490
2	820	−723	−249	0	−183	−75	−511	−414
3	763	−705	−246	1	−64	−176	−488	−430
4	1089	−904	−293	0	−191	−115	−602	−417
5	1098	−922	−297	0	−108	−198	−606	−430
6	1093	−915	−294	0	−180	−125	−604	−426
7	1097	−925	−296	0	−119	−187	−606	−434
8	1095	−913	−295	0	−175	−132	−605	−423

[a] $E_{OI} = E_{a1} + E_{a2} + E_{b1} + E_{b2}$. [b] BDE $= E_{Pauli} + E_{electrostatic} + E_{OI}$.

Following the analysis of Re et al. on the $(CO)_5CrC_nH_2$ series,[20a] we have carried out a fragment analysis which includes an FMO population analysis and the decomposition of the bonding energy between the fragments in the way proposed by Ziegler et al.[31] The bond dissociation energy (BDE) corresponding to the formation of the C_nH_2 and $[Cl(PH_3)_4Ru]^+$ fragments considered in their lowest singlet state from a $[Cl(PH_3)_4RuC_nH_2]^+$ molecule is decomposed into an electrostatic term, a Pauli repulsion term, and the different irreducible representation contributions to the orbital interaction energy. In simple MO theory, the Pauli repulsion term is approximated as the result of the four-electron/two-orbital destabilizing interactions, whereas the orbital interaction term results from the two-electron/two-orbital bonding interactions.[32] Our computed results are reported in Table 1. In these calculations, geometries of the isolated fragments were not allowed to relax and the constraint of ideal C_{2v} symmetry was applied, so that the b_1 and b_2 irreducible representations correspond to the $\pi_{||}$ and $\pi_{\perp}$ orbitals, respectively. Our computed data follow qualitative trends similar to those obtained by Re et al. on the $(CO)_5CrC_nH_2$ series.[20a] With the exception of the $n = 1$ special case, the BDE, which corresponds to the sum of the steric and the orbital interaction terms, varies weakly with n. It is slightly larger for complexes with $n =$ odd than for complexes with $n =$ even.

As can be deduced from the above description of the π-type interactions, when n is odd, the b_2 ($\pi_{\perp}$) contribution to the orbital interaction energy is larger than the b_1 ($\pi_{||}$) component, whereas the opposite situation occurs when n is even. The sum of the b_1 and b_2 π-type contributions exhibits odd/even oscillations which are consistent with the oscillations of the Ru−C distances

(31) (a) Ziegler, T.; Rauk, A. *Theor. Chim. Acta* **1977**, *46*, 1. (b) Ziegler, T. *NATO ASI Ser.* **1986**, *No. C176*, 189.
(32) (a) Rosa, A.; Baerends, E. J. *New J. Chem.* **1991**, *15*, 815. (b) Landrum, G. A.; Goldberg, N.; Hoffmann, R. *J. Chem. Soc., Dalton Trans.* **1997**, 3605.

Table 2. HOMO and LUMO Localization and Atomic Net Charges Computed for the $[Cl(PH_3)_4RuC_nH_2]^+$ Series

n		Cl	Ru	total C	C(1)	C(2)	C(3)	C(4)	C(5)	C(6)	C(7)	C(8)
1	HOMO %	53	42	0	0							
	LUMO %	2	27	62	62							
	net charge	−0.43	0.69	−0.17	−0.17							
2	HOMO %	39	38	23	3	20						
	LUMO %	2	20	61	59	2						
	net charge	−0.46	0.66	−0.12	−0.26	0.14						
3	HOMO %	30	40	26	6	20	0					
	LUMO %	3	18	75	32	6	37					
	net charge	−0.44	0.60	−0.10	−0.28	−0.03	0.21					
4	HOMO %	23	32	43	6	17	2	18				
	LUMO %	2	15	73	34	3	35	1				
	net charge	−0.45	0.60	−0.10	−0.31	−0.05	0.07	0.19				
5	HOMO %	18	31	47	8	17	4	17	1			
	LUMO %	2	14	82	22	5	23	3	29			
	net charge	−0.45	0.61	−0.09	−0.34	−0.06	0.03	0.04	0.24			
6	HOMO %	13	26	60	8	14	3	15	2	18		
	LUMO %	2	12	79	23	3	25	2	26	0		
	net charge	−0.45	0.60	−0.08	−0.34	−0.08	0.03	0.01	0.11	0.19		
7	HOMO %	11	25	60	9	14	5	14	3	15		
	LUMO %	2	12	85	16	3	17	3	20	2	24	
	net charge	−0.45	0.61	−0.07	−0.35	−0.09	0.00	0.01	0.07	0.06	0.23	
8	HOMO %	10	22	68	8	12	4	12	2	13	2	15
	LUMO %	2	10	82	17	4	18	2	20	1	20	0
	net charge	−0.45	0.61	−0.04	−0.34	−0.09	0.00	−0.01	0.07	0.03	0.10	0.20

and of the HOMO/LUMO gap. However these oscillations tend to vanish when *n* increases, so that the sum of the b_1 and b_2 contributions remains almost constant when $n > 3$. A similar situation occurs for the a_1 (σ-type) contribution, so that the total orbital interaction term is also almost constant for $n > 3$. Conversely, the Pauli and electrostatic terms exhibit odd/even oscillations which are out of phase. However, the amplitudes of the oscillations of the electrostatic term are larger, so that they dominate the total bonding energy (Table 1). Consequently, complexes with n = odd appear somewhat to be more thermodynamically stable than complexes with n = even. This may explain why only complexes with $n = 3, 5$ have been prepared so far.

The Mulliken atomic net charges computed for the $[Cl(PH_3)_4RuC_nH_2]^+$ series are given in Table 2. The variation of the carbon charges along the C_n chains exhibits qualitative trends similar to those of the $(CO)_5CrC_nH_2$ series.[20a] However, the carbon atom bonded to the metal is significantly more negatively polarized in the ruthenium series. This is due to the presence of the π-donor chloride ligand trans to the cumulenic chain. On the other hand, the terminal carbon is more positively polarized in the ruthenium series. The percentage localization of the HOMOs and LUMOs of the $[Cl(PH_3)_4RuC_nH_2]^+$ series along the $ClRuC_n$ chain is also given in Table 2. These values are close to those obtained by Re et al. for the $(CO)_5CrC_nH_2$ series,[20a] indicating that the electron donor effect of the chloride ion is spread out over several occupied MOs. It is also important to note that the HOMOs of the ruthenium compounds have some chlorine character. As *n* increases, the contributions of the C_n chain to the HOMO and LUMO increase, whereas the Ru and Cl contributions decrease. The localization of the LUMO along the carbon chain suggests that an orbital-controlled nucleophilic attack should occur at C(odd) atoms. On the other hand, arguments based on charge control strongly disfavor C(1) as a nucleophilic attack site. This is in agreement with the experimental finding on $[Cl(dppe)_2RuC_3Ph_2]^+$ and $[Cl(dppe)_2RuC_5Ph_2]^+$, which have been shown to react with nucleophiles at C(3) and C(5) but not at C(1).[4−6] In these complexes, the nonreactivity of C(1) can also be interpreted as resulting from the steric protection by the dppe ligands.

The HOMO localization favors the C(even) atoms for an orbital-controlled electrophilic attack, whereas arguments based on charge control strongly disfavor the distal carbon atom, even in the case of even chains. However, both conclusions are consistent with the observation of C(2) as being the protonation site in $[Cl(dppe)_2RuC_3MeR]^+$ (R = Ph, Me, H).[33] Rather similar conclusions on the electrophilic attack sites were found by Koentjoro et al. in their calculations on Ru^{II} polyynyl complexes.[22]

2. The $Cl(PH_3)_4RuC_nH_2$ Series. Compounds of the type $[Cl(dppe)_2RuC_nPh_2]^+$ ($n = 3, 5$) have been shown by cyclic voltammetry to undergo two one-electron reduction waves, the first one being reversible. Moreover, the corresponding $Cl(dppe)_2RuC_nR_2$ ($n = 3, 5$) neutral species have been spectroscopically (EPR) and chemically characterized in solution, although not isolated in the solid state, so far.[5−8] This is why we have undertaken DFT calculations on the $Cl(PH_3)_4RuC_nH_2$ ($n = 1−8$) series. From simple Lewis theory, the two-electron reduction of a $[Cl(dppe)_2RuC_nR_2]^+$ complex is expected to lead to canonical formulas indicating some sp^2 or (terminal) sp^3 carbon atoms. Thus, assuming that the $[Cl(dppe)_2RuC_nR_2]^-$ anion is stable, some bending of its C_n chain, possibly associated with some pyramidalization of the terminal carbon atom, may be anticipated. By interpolation, the one-electron reduction of $[Cl(dppe)_2RuC_nR_2]^+$ is also expected to induce some, although less pronounced, bending or pyramidalization. Surprisingly, full geometry optimization without any symmetry constraint yielded geometries of pseudo-C_{2v} symmetry with linear C_n chains and planar coordination for the terminal tricoordinated carbon (i.e. similar to those of their cationic relatives), with the exception of

(33) Touchard, D.; Rigaut, S. Unpublished results.

Table 3. SOMO Localization, Spin Density, and Atomic Net Charges Computed for the $Cl(PH_3)_4RuC_nH_2$ Series

n		Cl	Ru	total C	C(1)	C(2)	C(3)	C(4)	C(5)	C(6)	C(7)	C(8)
1	SOMO %	3	25	64	64							
	spin density	0	0.05	1.03	1.03							
	net charge	−0.56	0.64	−0.19	−0.19							
2	SOMO %	5	26	54	54	0						
	spin density	0.03	0.14	0.67	0.79	−0.12						
	net charge	−0.57	0.67	−0.26	−0.32	0.06						
3	SOMO %	2	13	81	34	6	41					
	spin density	0	0.05	1.02	0.49	−0.16	0.69					
	net charge	−0.56	0.64	−0.38	−0.33	−0.10	0.05					
4	SOMO %	1	10	78	36	3	38	1				
	spin density	0	0.04	0.84	0.54	−0.18	0.61	−0.13				
	net charge	−0.55	0.65	−0.44	−0.38	−0.11	−0.05	0.10				
5	SOMO %	1	10	87	23	5	24	3	32			
	spin density	0	0.04	1	0.32	−0.11	0.39	−0.17	0.57			
	net charge	−0.55	0.65	−0.46	−0.37	−0.13	−0.06	0	0.10			
6	SOMO %	1	8	84	24	3	27	2	28	0		
	spin density	0	0.04	0.87	0.37	−0.13	0.44	−0.17	0.48	−0.12		
	net charge	−0.54	0.65	−0.49	−0.38	−0.13	−0.07	−0.03	0.01	0.11		
7	SOMO %	1	8	90	17	3	18	3	21	2	26	
	spin density	0	0.04	1	0.24	−0.08	0.29	−0.13	0.36	−0.17	0.49	
	net charge	−0.54	0.65	−0.52	−0.37	−0.15	−0.07	−0.03	−0.02	0.01	0.11	
8	SOMO %	1	7	87	18	3	19	2	22	1	22	0
	spin density	0	0.04	0.88	0.28	−0.10	0.33	−0.15	0.39	−0.16	0.40	−0.11
	net charge	−0.54	0.64	−0.53	−0.37	−0.14	−0.08	−0.04	−0.02	−0.02	0.02	0.12

$Cl(PH_3)_4RuC_2H_2$, in which the Ru−C(1)−C(2) angle is 146° (see Figure 1).

The major bond distances in the $Cl(PH_3)_4RuC_nH_2$ radicals are given in Figure 2. Comparing these data to those of the corresponding cations, a lengthening of most of the bond distances can be noted. From this point of view, it is noteworthy that the Ru−Cl bond length increases significantly upon reduction but decreases with *n*. This is consistent with the Ru−Cl antibonding character of the $[Cl(PH_3)_4RuC_nH_2]^+$ LUMO (Table 2), which decreases with *n* as well. On the other hand, some of the C−C bonds are shortened upon reduction. In particular, the C(1)−C(2) bond is shorter by ∼0.02 Å in the reduced form in all of the complexes, except when this bond is the terminal one. The C(3)−C(4) bond is also shortened, but more slightly, when $n > 4$, as well as the C(5)−C(6) bond when $n > 6$. Thus, the general tendency is a shortening of the C(odd)−C(even) bonds, providing they are not the terminal C−C bond of the chain. This shortening is rapidly damped when the C−C bond moves away from the metal. This effect is consistent with the bonding character of the considered bonds in the $[Cl(PH_3)_4RuC_nH_2]^+$ LUMO. Thus, there is a tendency toward some carbyne-type character of the part of the chain which is close to the metal. These theoretical calculations are consistent with the experimental data, which indicate significant localization of the single electron on the terminal carbon.[6] It is noteworthy that this effect is also present in $Cl(PH_3)_4RuC_2H_2$, despite the 146° bending at C(1). Calculations on $Cl(PH_3)_4RuC_2H_2$ assuming C_{2v} symmetry (i.e. a linear C_2 chain) lead to an energy which is only 0.012 eV higher than that of the bent structure with very similar bond lengths.

The Mulliken net charges and spin densities computed for the $Cl(PH_3)_4RuC_nH_2$ series are given in Table 3, together with the percentage of localization of the singly occupied molecular orbital (SOMO). For all the computed models, this latter orbital is very similar to the LUMO of the corresponding cation (compare Tables 2 and 3).

The major change occurring upon populating this orbital with one electron is a small decrease of its metal localization at the expense of the C_n chain. Interestingly, although the $Cl(PH_3)_4RuC_nH_2$ SOMO still has some significant Ru localization, there is very little spin density on the metal (Table 3), even in the case of $n = 1$. Clearly, the occupation of the $[Cl(PH_3)_4RuC_nH_2]^+$ LUMO induces significant electronic and spin relaxation. Thus, the one-electron reduction of the $[Cl(PH_3)_4RuC_nH_2]^+$ cations affects primarily the C_n chain, so that the $Cl(PH_3)_4RuC_nH_2$ species are better described as 18-electron Ru^{II} centers bonded to a radical $(C_nH_2)^-$ ligand rather than their being 19-electron complexes.

The calculations are in full agreement with EPR measurements and hydrogen capture experiments on the reduced species, which indicate localization of the single electron on the C_n chain.[6]

The adiabatic ionization potentials of the $Cl(PH_3)_4RuC_nH_2$ ($n = 1-8$) compounds, calculated as the energy difference between the neutral and cationic species, are shown in Figure 5. The plot shows odd/even oscillations, indicating that the neutral radicals having an odd number of carbon atoms are more difficult to oxidize: i.e., the corresponding cations are easier to reduce. The oscillations are damped as *n* increases, and the ionization potential tends to an asymptotic value of ∼6 eV. These oscillations are consistent with the simple view of oxidizing a $(C_nH_2)^-$ ligand bonded to a Ru^{II} center since, as a consequence of topology, the HOMO of $(C_nH_2)^-$ when *n* is odd is expected to lie at a lower energy than that of $(C_{n+1}H_2)^-$.

3. The $[Cl(PH_3)_4RuC_nH_2]^-$ Series. As stated above, cyclic voltammetry of the compounds $[Cl(dppe)_2RuC_nR_2]^+$ ($n = 3, 5$) exhibits two one-electron reduction waves. In contrast to the first wave, the second one is irreversible. To investigate the stability and properties of the bireduced states of the cationic species, we have also undertaken DFT calculations on the $[Cl(PH_3)_4RuC_nH_2]^-$ ($n = 1-8$) series. The anions corresponding to $n = 1, 2$ were found to be unstable with respect to phosphine dissociation. Anions with longer carbon chains were

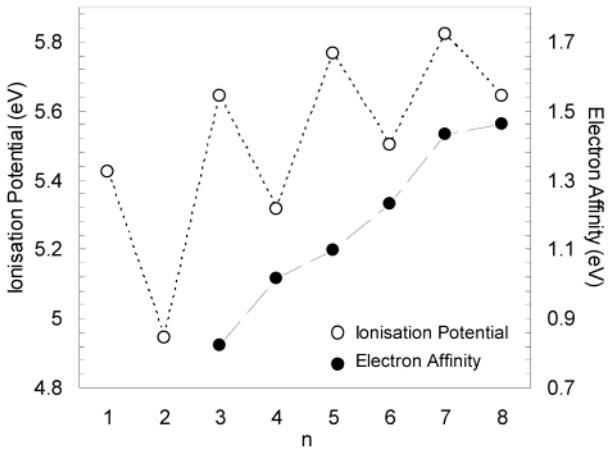

Figure 5. Computed adiabatic ionization potentials and electron affinities (in eV) plotted as a function of *n* for the $Cl(PH_3)_4RuC_nH_2$ series.

found to be stable, with their lowest singlet and triplet states lying close in energy. In all the cases the singlet state is computed to be the ground state, by 0.02, 0.08, 0.06, 0.04, 0.17, and 0.09 (in eV) for $n = 3-8$, respectively. The geometry optimizations of both spin states were carried out without any symmetry constraint. The optimized singlet state geometries are close to the ideal C_s symmetry, as exemplified by the structures of $[Cl(PH_3)_4RuC_7H_2]^-$ and $[Cl(PH_3)_4RuC_8H_2]^-$, which are shown in Figure 1. They are all significantly bent at C(1), with bending angles equal to 132, 119, 126, 133, 138, and 128° for $n = 3-8$, respectively. This bending is associated with a rather short C(1)−C(2) separation, as can be seen in Figure 2, which shows the bond distances optimized for the singlet state of the anionic series. On the other hand, the Ru−C(1) distance is significantly longer in the anion as compared to the cation (Figure 2). There is no pyramidalization of the terminal carbon in the anions. In the case of the odd-carbon chains, the CH_2 plane is perpendicular to the plane defined by Ru, C(1), and C(2), whereas it lies in this plane in the case of the even chains (see the $n = 7$ and $n = 8$ examples in Figure 2). This structural behavior is indicative of an allenic type of the carbon chain.

The optimized triplet state geometries are not significantly different from C_{2v} symmetry, with linear C_n chains, as in the cationic series. The corresponding bond distances are provided in Table S1.

The electron affinities of the $Cl(PH_3)_4RuC_nH_2$ ($n = 3-8$) compounds, calculated as the energy difference between the ground states of the anionic and neutral species, are plotted with respect to *n* in Figure 5. As for the ionization potentials, the electron affinity increases with *n*, but without significant odd/even oscillations.

The computed atomic net charges are provided in Table S2 for both singlet and triplet states. The singlet state has a more negative C(1) atom and a more positive metal than its triplet counterpart. This is in agreement with the bending of the singlet state geometry at C(1), which is indicative of a reduced, formally $(C_nH_2)^{2-}$, carbon chain bonded to an 18-electron metal center.

Summary and Conclusion

Analysis of the electronic structure of the 18-electron $[Cl(PH_3)_4RuC_nH_2]^+$ model complexes indicates that the linear C_nH_2 ligand is somewhat more strongly bonded to the $[Cl(PH_3)_4Ru]^+$ unit when $n =$ odd, in agreement with the fact that no $n =$ even complexes have been isolated so far. The distribution of the atomic net charges and the localization of the HOMOs and LUMOs indicate that the complexes are subject to nucleophilic attack at C(odd) atoms, except in the case of C(1). They are subject to electrophilic attack at the C(even) sites, except when it is the CH_2 end of the chain. These findings are in agreement with all the experimental data available so far on related compounds.[4−6,33]

The one-electron reduction of the $[Cl(PH_3)_4RuC_nH_2]^+$ compounds leads to neutral species presenting linear C_nH_2 chains, with the exception of the $n = 2$ complex, which is bent at C(1). In agreement with available experimental data,[6] the $Cl(PH_3)_4RuC_nH_2$ compounds are better described as 18-electron Ru^{II} metals bonded to reduced $(C_nH_2)^-$ ligands rather than 19-electron Ru^I centers. The $[Cl(PH_3)_4RuC_nH_2]^+$ complexes are found to be easier to reduce when $n =$ odd rather than when $n =$ even.

The two-electron reduction of the $[Cl(PH_3)_4RuC_nH_2]^+$ compounds leads to anions which are found stable with respect to ligand dissociation only when $n > 2$. Their ground state was found to be a singlet presenting significant bending at C(1). This bending allows the extra charge localization on C(1) and tends to preserve the metal 18-electron configuration. The lowest triplet state lies close in energy to the singlet state and exhibit linear C_nH_2 chains.

Acknowledgment. We are grateful to Prof. M. I. Bruce (University of Adelaide) for helpful comments and criticisms. Computing facilities were provided by the Centre de Ressources Informatiques (CRI) of Rennes and the Institut de Développement et de Ressources en Informatique Scientifique du Centre National de la Recherche Scientifique (IDRIS-CNRS).

Supporting Information Available: Triplet state bond distances (Table S1) and atomic net charges for the singlet and triplet states of $[Cl(PH_3)_4RuC_nH_2]^-$ series (Table S2). This material is available free of charge via the Internet at http://pubs.acs.org.

OM020543C